CROPLAND OBSERVATORY NODES (CRONOS): PORTABLE, INTEGRATED SOIL-PLANT-ATMOSPHERE MONITORING SYSTEMS

By

D. COLE DIGGINS

Bachelor of Science in Soil, Plant, and Atmospheric Sciences

University of Missouri

Columbia, Missouri

2020

Submitted to the Faculty of the
Graduate College of the
Oklahoma State University
in partial fulfillment of
the requirements for
the Degree of
MASTER OF SCIENCE
July, 2022

CROPLAND OBSERVATORY NODES (CRONOS):

PORTABLE, INTEGRATED SOIL-PLANT-

ATMOSPHERE MONITORING SYSTEMS

Thesis Approved:

Thesis Adviser – Tyson Ochsner

Brian Arnall

Eric Benton

ACKNOWLEDGEMENTS

We would like to thank the USDA NIFA Agriculture and Food Research Initiative for funding the Rainfed Agriculture Innovation Network project which supported this study. Thank you to our farmer cooperators and the Oklahoma State University South Central Research Center for allowing us to deploy our stations at sites across Oklahoma. Thank you to William G. Brown, Madison Morris, and Samantha Burns for their work on the project, assisting with much of the fieldwork and labor. In addition, a thank you to Evens Robert and Connor Colby for their work to build upon some of the findings of this study.

Name: D. Cole Diggins

Date of Degree: JULY, 2022

Title of Study: CROPLAND OBSERVATORY NODES (CRONOS): PORTABLE, INTEGRATED SOIL-PLANT-ATMOSPHERE MONITORING SYSTEMS

Major Field: PLANT AND SOIL SCIENCES

Abstract: In croplands the conditions within the soil-plant-atmosphere continuum can differ substantially from those at the closest available weather station, thus there is a need for monitoring stations optimized for deployment in cropland. Developed in response to this need, CRopland Observatory NOdeS (CRONOS) are portable in-situ, multi-sensor monitoring stations designed to monitor soil water content, green canopy cover (GCC), and atmospheric conditions. The objective of this study was to evaluate the performance of first-generation CRONOS systems on working farms. During the 2020-2021 winter wheat (*Triticum aestivum*) growing season, CRONOS stations were installed at three sites across Oklahoma, USA. Each station was equipped with a cosmic-ray neutron sensor to measure soil moisture, a camera to monitor GCC, and an all-in-one weather station. The soil moisture estimates were validated by comparison with distance- and depth-weighted average volumetric water content determined by soil sampling. The station's GCC estimates were compared with the average GCC at the field scale. Meteorological data from the all-in-one weather stations were compared with observations from the Oklahoma Mesonet closest to each CRONOS site. The CRONOS stations accurately determined field-average soil water content, with a mean average difference (MAD) of 0.022 cm^3cm^{-3} and a Nash-Sutcliffe Efficiency (NSE) of 0.756. The CRONOS GCC estimates showed greater discrepancies from the field-scale averages than did the soil water content estimates, with a MAD of approximately 12% and NSE of 0.43. These differences were most pronounced at one site where the crop growth near the station was less representative of the field as a whole. For atmospheric conditions, the level of agreement between the measurements of the CRONOS stations and the nearest Mesonet station varied, with NSE values ≥ 0.89 for measurements of air temperature, solar radiation, and atmospheric pressure but lower NSE values ranging from 0.34 – 0.87 for precipitation, relative humidity, and wind speed. Sensors were found to be reliable $\geq$ 98.4% percent of the time except for the cameras, for which 18.5% of the scheduled photos were missing. For subsequent generations of CRONOS stations, development efforts should focus on identifying more reliable and representative vegetation monitoring.

TABLE OF CONTENTS

Chapter Page

I. INTRODUCTION 1

II. MATERIALS AND METHODS 4

2.1 Study Area 4
2.1.1 Site Soil Properties 5
2.2 CRONOS Configuration 5
2.2.1 Soil moisture measurements 6
2.2.2 Plant measurements 9
2.2.3 Atmospheric measurements 9
2.3 Validation 10
2.3.1 Soil moisture and green canopy cover validation 10
2.3.2 Atmospheric measurements validation 11
2.3.3 Reliability assessment 11

III. RESULTS AND DISCUSSION 13

3.1 Accuracy of the Soil Moisture Data 13
3.2 Accuracy of the Green Canopy Cover Data 15
3.3 Accuracy of the Weather Data 17
3.4 Sensor Reliability 18
3.5 Limitations 20

IV. CONCLUSIONS 21

REFERENCES 23

APPENDICES 26

LIST OF TABLES

Table Page

1 Agronomic and climatological data for each site where CRONOS stations were deployed. 26

2 The average bulk density, porosity, and volumetric water content at wilting point (-1500 kPa) at each depth, for each CRONOS site. 27

3 The MAD, NSE, and percent bias of each CRONOS station variable when compared to the nearest Oklahoma Mesonet station on a by variable basis. θ is the soil moisture, and P is the sum of daily precipitation. T_{max} and T_{min} are the daily maximum and minimum temperature. R_s is the daily sum of the solar flux density. RH_{max} and RH_{min} are the daily maximum and minimum relative humidity. P_a is the atmospheric pressure. u_2 is the daily average wind speed and Dis. indicates the distance between the CRONOS and Mesonet stations.....28

LIST OF FIGURES

Figure Page

1 The location of the three CRONOS sites utilized in this study. The small inlaid map shows Oklahoma's location within the United States and the coloration of the map indicates the predominant land cover type throughout the state. The CRONOS stations are distributed so that they span much of the winter wheat growing region of Oklahoma. 29

2 Photograph of CRONOS station 2 located in Tillman County, Oklahoma near the town of Chattanooga. This station is equipped with an all-in-one weather station (top), digital camera (arm), and cosmic ray neutron detector (box) which is located behind the data logger (box). 30

3 Time series of the smoothed hourly soil moisture (cm^3cm^{-3}) from each CRONOS station during the 2020-2021 winter wheat growing season. The red diamonds represent the distance- and depth-weighted average soil moisture of the field as determined by periodic soil sampling. The error bars on the diamonds represent the standard deviation of soil sampling. The dashed magenta line represents the depth-weighted daily soil moisture measured at the Mesonet site nearest to each CRONOS station. The red bars at the base of each plot represent CRONOS daily precipitation totals throughout the course of the growing season. 31

4 CRONOS soil moisture data versus field-scale average soil moisture estimated based on soil samples collected at different times throughout the growing season at a total of 14 locations on concentric circles with radii of 5, 50, and 100 m around the CRONOS station. The CRONOS data are the average of the 4 hours after the start of soil sampling, and the hourly data were smoothed with a Savitzky-Golay filter. The soil moisture values for each soil sampling location and depth (0-5, 5-10, 10-40 cm) were weighted according to the procedure of Köhli et al. (2015) to calculate the field-scale average 32

5 Daily average green canopy cover (GCC) measured using photos from a digital camera measured mounted on the CRONOS station. The photos were processed using the Canopeo algorithm (Patrignani and Ochsner, 2015) to determine GCC. The red crosses are the field-scale average GCC based on 14 photographs taken at the soil sampling locations using a smartphone, and the red bars are the standard deviation of this data set. Images were processed by the Canopeo smartphone application. 33

6 CRONOS green canopy cover (GCC) estimate plotted against the field-scale average GCC based on measurements at 14 locations in each field on five dates throughout the growing season. The CRONOS GCC values are the average GCC for the photos collected by the station at five times (09:00, 11:00, 13:00, 15:00, and 17:00) on the day of sampling. The MAD, NSE, and bias across all three sites are displayed in the top left corner. 34

7 Time series of daily maximum (blue) and minimum (red) air temperatures at each CRONOS station, along with the daily maximum and minimum air temperature measured by the closest station of the Oklahoma Mesonet. ..35

8 Percent of missing or invalid sub-daily observations for CRONOS atmospheric variables, GCC readings, and soil moisture (θ) measurements across three sites in Oklahoma during the 2020-2021 winter wheat growing season. P is precipitation. T air temperature. R_s is solar radiation. RH is relative humidity. P_a is atmospheric pressure. P_v is vapor pressure. u_2 is wind speed at 2 m, and GCC is the green canopy cover.....36

CHAPTER I

INTRODUCTION

Farmers and researchers require accurate, real-time, field-scale information about conditions within the soil-plant-atmosphere continuum to make informed cropland management decisions, to predict crop yields, and to evaluate and improve models and remote sensing algorithms for cropland. This need is especially great for soil moisture data because it fundamentally influences agricultural and land surface processes, but it is difficult to monitor in fields that are actively being farmed. Thus, accurate field-scale soil moisture information for cropland is rarely available. Instead, farmers may estimate soil moisture conditions based on experience and intuition considering recent weather conditions, or they may rely on state (McPherson et al., 2007) or national (Quiring et al., 2016) monitoring networks to represent soil moisture conditions, perhaps not realizing that the data from such networks rarely reflect cropland soil moisture conditions (Patrignani and Ochsner, 2018). Likewise, in the absence of field-scale cropland soil moisture data, scientists are limited in their ability to evaluate remotely sensed soil moisture products (Colliander et al., 2019). Similarly, the lack of data on green canopy cover dynamics in cropland can hinder the development and evaluation of models for crop evapotranspiration (Pereira et al., 2020).

Soil moisture observations can help inform agricultural management decisions and have been used to improve yield predictions from crop models (Krueger et al., 2021). Also, by

combining measurements of soil water content with hydrologic models, researchers have accurately predicted seasonal streamflow and estimated potential groundwater recharge (Wyatt et al., 2017, Wyatt et al., 2020). For these and other applications, using a sensor with a relatively large support volume may be beneficial if the sensor can effectively average the spatial heterogeneity of soil water content in the field of interest. One promising proximal sensing approach to accurately monitor field-scale soil volumetric water content uses cosmic-ray neutron detectors (Desilets et al., 2010). These detectors count high-energy fast neutrons approximately 1 m above the soil surface, and the fast neutron count rate is inversely related to the soil water content of the surrounding soil out to ~200 m radius (Köhli et al., 2015). The effective sensing depth for this method varies with soil water content, ranging from ~15 cm for soil near saturation to ~80 cm for completely dry soil (Köhli et al., 2015). However plant biomass also influences the fast neutron counts, thus changes in the plant biomass, such as those associated with the growth and harvest of crops, may introduce errors in the soil water content estimates (Iwema et al., 2021).

Along with soil water content observations, cropland vegetation monitoring can also benefit farmers and researchers by enabling them to quantitatively track the growth of the crop over time. Remote monitoring of crop growth may be particularly helpful for fields located far from the farm headquarters for which daily or weekly visits may prove difficult. Measurements of green canopy cover (GCC) provide a good indicator of crop water use and evapotranspiration partitioning (Yimam et al., 2015). The GCC of crops can be nondestructively monitored by analyzing downward-facing digital images taken from above the crop canopy using the Canopeo algorithm (Patrignani and Ochsner, 2015). However, long-term, unattended GCC monitoring systems have not been adequately developed or evaluated.

In contrast, meteorological monitoring systems for cropland are relatively well developed. The site-specific meteorological data from such systems are useful, for tracking key

variables such as growing season precipitation, and for daily cropland management decisions, such as whether wind speed and direction are suitable for herbicide application. There are many sources of weather data available, such as state Mesonets, the best of which have approximately 40 km between neighboring stations (Ochsner et al., 2013). At that distance the inherent spatial variability of precipitation can lead to large differences in the local precipitation totals (Rossel and Garbrecht, 1999). Thus, there is continued interest in site-specific weather data, and technological advancements have enabled the development of relatively low cost, compact, all-in-one weather stations that may be well suited for cropland monitoring (Schunke et al., 2021, Dombrowski et al., 2021). However, evaluations of these all-in-one compact weather stations are limited, and the long-term accuracy and reliability in the context of cropland monitoring is unknown.

With their compact size and diverse array of measurements, the first generation CRONOS stations, introduced here, may be appealing to farmers and researchers, but the complete system has not been previously field tested, and uncertainties exist regarding the data accuracy, representativeness, and reliability in cropland environments. Therefore, our objective was to evaluate the performance of the CRONOS stations on working farms during the 2020-2021 winter wheat growing season at three sites in Oklahoma, USA. The accuracy of soil moisture measured using the cosmic-ray neutron detectors was assessed by comparing readings with field-scale soil volumetric water content measurements, canopy cover data were evaluated by comparison with the average green canopy cover of the field at selected times throughout the growing season, and the weather measurements were evaluated by comparing them with the measurements of the nearest permanent weather station.

CHAPTER II

MATERIALS AND METHODS

Study Area

We evaluated the performance of CRONOS stations at three locations representative of Oklahoma's wheat producing region: station 1 was installed in Grady County near the town of Chickasha, station 2 in Tillman County near the town of Chattanooga, and station 3 in Kay County near the town of Braman (Figure 1). The soil at the Chickasha site was mapped as a McLain silty clay loam (fine, mixed, superactive, thermic Pachic Argiustoll) on 0 to 1 percent slopes, rarely flooded (Soil Survey Staff, 2022). This site was located on the Oklahoma State University South Central Research Center. All sites were planted with winter wheat (*Triticum aestivum*) and agronomic data can be found in Table 1 (Oklahoma, 2022). The soil at the Chattanooga site was mapped as Indiahoma silty clay loam (fine, smectitic, thermic Typic Haplustert) on 1 to 3 percent slopes. This site was located on a cooperating farm and grazed by beef cattle at a moderate stocking density from approximately November 25, 2020 to February 15, 2021. The soil at the Braman site was mapped as Milan loam (fine-loamy, mixed, superactive, thermic Udic Argiustoll) on 0 to 1 percent slopes. This site was located on a cooperating farm. The data used in this study were collected between Oct. 1, 2020 and Jun. 17, 2021, which spanned the winter wheat cropping season at each site.

Site soil properties

The physical properties of the soil at each of CRONOS site was determined by soil sample analysis. The average bulk density, porosity, and wilting point were analyzed for each depth at each site (Table 2). The bulk density and the porosity were determined using the core method (Gavlak et al., 2003). The volumetric water contents at wilting point (-1500 kPa) were determined using the pressure plate method (Madsen et al., 1986).

CRONOS Configuration

The CRONOS stations were equipped with a cosmic-ray neutron detector to measure soil moisture, a downward-facing digital camera to monitor plant canopy growth, and an all-in-one weather station (Figure 2). The evaluation of the CRONOS stations included four parts, first evaluating the accuracy of each measurement type (soil, plant, and atmosphere) by comparing them with independent measurements and then analyzing the reliability of the stations as reflected by the percent of missing or out of range data for each management type.

The stations were built using a 183-cm tall tripod (QST6, Campbell Scientific, Logan, UT) as the main frame, equipped with adjustable leg angles and feet with holes to insert anchors. The metal anchors (PE-T9, American Earth Anchors, Woonsocket, RI) were 23-cm long with a corkscrewed flight diameter of 2.8-cm and were screwed into the ground by hand or with the assistance of a wrench to gain leverage. To facilitate precise leveling of the all-in-one weather station, we developed an adjustable mount for the top of the tripod consisting of two horizontal parallel plates with leveling screws on each corner of the top plate. On the bottom plate, metal loops were welded to attach guy-wires from the feet of the station in order increase stability. The CRONOS stations were powered by 12-volt marine batteries placed at the base of each station and recharged by south-facing 30-W solar panels.

Soil moisture measurements

Soil moisture was monitored using a cosmic-ray neutron sensor (CRS1000, Hydroinnova, Albuquerque, NM) which uses a ^{3}He-filled tube for neutron detection. When slow (or thermal) neutrons interact with the ^{3}He gas inside the detector, an electrical charge is built up and discharged along an internal copper wire where it is detected by an attached pulse module (RPM 1000, Questa, Los Alamos, NM) as a neutron count and recorded by a datalogger (DL- 2100, Questa, Los Alamos, NM). The neutron detection tube is encased in 2.54 cm of high-density polyethylene, to slow (or thermalize) incoming fast neutrons and prevent incoming slow neutrons from being detected (Zreda et al., 2012). Because fast neutrons are slowed most effectively by interactions with hydrogen atoms, the most common environmental source of which is water, a decrease in the fast neutron counts is associated with an increase in soil moisture. The cosmic-ray neutron detector is sensitive to soil moisture within a circular footprint with a radius that ranges from 130-240 m and a depth that typically ranges from approximately 10-40 cm (Köhli et al., 2015). The effective sensing depth decreases as the soil moisture increases.

Multiple factors in addition to soil moisture can influence the fast neutron counts, and the neutron counts must be corrected to account for the influence of these factors in order to accurately estimate soil moisture (Andreasen et al., 2017). The largest correction factor accounts for variation in the atmospheric pressure, because an increase in atmospheric pressure indicates an increased mass per unit area of atmospheric molecules that incoming fast neutrons must travel through before reaching the land surface (Badiee et al., 2021). This correction factor f_p is described as

$$f_P = e^{(P_0 - P_a)/L} \quad \text{[Eq.1]}$$

where f_P represents the atmospheric pressure correction, L represents the mass attenuation length of high energy neutrons (130 mbar) (Zreda et al., 2012). P_a represents the observed atmospheric

pressure (mbar) during neutron count collection and P_0 is the reference atmospheric pressure (1013.25 mbar). Changes in atmospheric vapor pressure also influence the neutron counts because increasing vapor pressure indicates an increase in the amount of water present in the atmosphere and thus an increase in environmental hydrogen, which thermalizes cosmic ray neutrons. The vapor pressure correction factor, f_h, is:

$$f_h = 1 + 0.0054(h - h_0) \quad \text{[Eq. 2]}$$

where f_h represents the humidity correction, h represents the absolute humidity (g m^{-3}) derived from the temperature and relative humidity detected by CRONOS, and h_0 represents the reference vapor density (0 g m^{-3}) (Rosolem et al., 2013). The third correction factor accounts for change in the incoming neutron flux, which for this study was estimated using data from the international Neutron Monitor Database for the station near Irkutsk, Russia (Sapundjiev et al., 2020). The incoming flux correction, f_I, is given by:

$$f_I = \frac{I}{I_0} \quad \text{[Eq. 3]}$$

where f_I is the correction of the neutron intensity, I is the hourly incoming neutron flux observed in Irkutsk, and I_0 is the daily mean incoming neutron flux at Irkutsk for the reference day, which was May 1, 2020. With all these correction factors defined, the corrected neutron count rate was calculated by:

$$N = \frac{N_{raw} \times f_h}{f_p \times f_i} \quad \text{[Eq. 4]}$$

where N is the corrected neutron count rate (counts per hour, cph), and N_{raw} represents the raw neutron count rate measured by the station (cph) (Andreasen et al., 2017), the average of which was approximately 850 cph. These corrected neutron counts are inversely related to the soil

volumetric water content. The relationship between soil moisture and the corrected counts can be represented as:

$$\theta = \left(\frac{a_0}{\frac{N}{N_0} - a_1} - a_2 - w_{lat} \right) \frac{\rho_b}{\rho_w} \qquad \text{[Eq. 5]}$$

where θ is the volumetric water content ($cm^3\ cm^{-3}$), ρ_b is the soil bulk density ($g\ cm^{-3}$), ρ_w is the water density ($0.998\ g\ cm^{-3}$), w_{lat} is the lattice water content of the soil ($g\ g^{-1}$), N_0 is a calibration factor which represents the neutron count rate over completely dry soil (cph), and the parameters $a_0 = 0.0808$, $a_1 = 0.372$ and $a_2 = 0.115$ (Desilets et al., 2010). Lattice water content was estimated as $0.03\ g\ g^{-1}$. The N_0 of each station was 1068.61 cph at Chickasha, 939.53 cph at Chattanooga, and 1112.79 cph at Braman. The bulk density (ρ_b) at each station was $1.53\ g\ cm^{-3}$ at Chickasha, $1.504\ g\ cm^{-3}$ at Chattanooga, and $1.50\ g\ cm^{-3}$ at Braman.

The cosmic-ray neutron detectors were calibrated using distance- and depth-weighted soil water content samples collected from the area surrounding each station (Köhli et al., 2015). These calibration samples were collected on Oct. 12, 2020, at Chickasha, Feb. 3, 2021, at Chattanooga, and Oct. 6, 2020, at Braman. Samples were collected along the circumference of concentric circles approximately 5, 50, and 100 m from each detector. Six samples were collected at the 5-m distance, four at 50 m, and four at 100 m. These samples were collected using a 3-cm diameter sample tube driven into the soil using a slide hammer (Giddings Machine Company, Windsor, CO) to a depth of 45 cm. These samples were divided into subsamples of 0-5 cm, 5-10 cm, and 10-40 cm in depth. The bulk density and soil water content of each sample were then determined by weighing before and after oven drying in the lab, and the distance- and depth-weighted average soil water content was calculated based on the spatial sensitivity of the neutron detector (Köhli et al., 2015). This water content value was then inserted into equation 5 along with the average corrected neutron count rate for the 4 hours starting at the beginning of the soil sample

collection period. The equation was then solved to determine N_0 for each station. Hourly soil moisture values were then calculated using the calibrated N_0 and smoothed using a third order Savitzky-Golay filter with a window length of 23 hours to reduce the noise within the estimated soil moisture data (Savitzky and Golay, 1964).

Plant measurements

To monitor crop canopy development, the CRONOS stations were equipped with a downward-facing camera (Range Cam 4G, Barn Owl, Colorado Springs, CO) that records RGB images and sends them via cellular modem to an ftp server for storage. The cameras were programmed to collect images daily at 9:00, 11:00, 13:00, 15:00, and 17:00 hours. The images were then processed using the Canopeo algorithm to determine the percent green canopy cover (Patrignani and Ochsner, 2015). The cameras were mounted on an aluminum tube that extended horizontally 1.2 m south from the central mast of the CRONOS station. The cameras were set at a height of 2 m, resulting in photographs encompassing approximately 6.0 m^2 at the ground surface. The images were 2560 x 1920 pixels (4.9 megapixels) in size requiring approximately 1.2 megabytes per image. Each pixel represents an area of about 1.2 mm^2 at the ground level.

Atmospheric measurements

CRONOS stations were also equipped with all-in-one weather stations (ClimaVue50, Campbell Scientific, Logan, UT) mounted 2.0 m above the ground. These compact units measure precipitation, air temperature, solar radiation, relative humidity, atmospheric pressure, wind speed, wind direction, vapor pressure, lightning strikes, and the average distance of those strikes (Campbell Scientific, 2019). Precipitation is measured using a drop counter rain gauge, using the conversion of 0.017 mm of rain per drop. Solar radiation is measured with a silicon-cell pyranometer engineered to be accurate regardless of sun angle. Wind speed and direction are measured using an ultrasonic anemometer. The device detects relative humidity and, using the

sensor temperature, the detected value is used to calculate the vapor pressure. Air temperature is measured using a shaded thermistor, with readings corrected for the effects of wind speed and solar radiation. The atmospheric pressure sensor measures the pressure imposed on the surface in the range of 500 to 1100 mbar. The all-in-one weather station is also equipped with a leveling bubble to help users properly deploy the system and bird spikes to prevent birds roosting on the precipitation funnel. The weather station was connected to the CRONOS data logger via SDI-12 protocol, and the weather data and neutron counts were transmitted hourly to an ftp server via the logger's internal cellular modem.

Validation

Soil moisture and green canopy cover validation

Soil moisture measurements from the cosmic-ray neutron detector were validated with additional soil samples that were collected in the same manner as the calibration samples. Samples were collected at 14 total locations on concentric circles 5, 50, and 100 m from each station five times over the 2020-2021 winter wheat growing season. The depth- distance-weighted average volumetric water content values determined by soil sampling were compared with the average soil moisture content detected by the station during the four-hour period following the start of the sampling process. The mean absolute difference (MAD) between the CRONOS soil water content and the soil water content determined by soil sampling was then calculated, along with the Nash-Sutcliffe Efficiency (NSE) (McCuen et al., 2006) and percent bias. Comparisons were also made between the soil water content determined by the nearest Oklahoma Mesonet station and that measured by the CRONOS stations. The Mesonet soil moisture values are estimated based on the matric potential measured using heat dissipation sensors (CS-229, Campbell Scientific, Logan, UT) installed at the 5-, 25-, and 60- cm depth (Zhang et al., 2019).

During the same five sampling dates for each site, downward-facing digital images were collected at each of the 14 soil sampling sites using a smartphone (G7 ThinQ, LG, Seoul, South Korea) held out at arm's length at chest height, prior to soil sample collection. Those images were processed to estimate green canopy cover (GCC) using "Foliage", a web implementation of the Canopeo algorithm (https://soilwater.ksu.edu/), and the average GCC of the field was calculated. The field average GCC was then compared with the daily average GCC of the CRONOS images collected that day to calculate the MAD, NSE, and percent bias of the CRONOS GCC values.

Atmospheric measurements validation

To assess the accuracy of the CRONOS weather data, measured weather variables were summarized by day and compared to daily data collected at the nearest Oklahoma Mesonet station (McPherson et al., 2007). Data accuracy was assessed using the MAD, NSE, and percent bias between the daily values for the CRONOS station and the Mesonet station. The CRONOS wind direction data were reported as the average direction observed over the course of each hour in degrees from north, whereas the Mesonet wind direction data were measured at a height of 10 m and reported as the most frequently detected direction for the day among the four cardinal directions, four intercardinal directions, and eight secondary intercardinal directions. Due to these technical differences, the comparison of wind direction data was omitted.

Reliability assessment

Missing and out-of-range data for each measurement type were flagged and removed from all statistical analysis. All neutron counts below 500 or above 1000 cph were considered out-of-range based on visual inspection of the data. Green canopy cover images were scheduled to be collected and transmitted five times each day, and all scheduled images not received by the ftp server were considered missing data. For the all-in-one weather station all out-of-range data were flagged by the station's firmware and denoted by either -9999 or -99 in the station's output.

CHAPTER III

RESULTS AND DISCUSSION

The first-generation CRONOS cropland monitoring stations were developed to help farmers and researchers better understand current soil-plant-atmosphere conditions relevant to their crops and management decisions, and this study provides the first report of field tests of the CRONOS stations on working farms. We compared soil moisture measurements from the CRONOS cosmic-ray neutron detectors and crop canopy cover measured using digital cameras, with independent, field-scale measurements at three locations in Oklahoma, USA. Weather data collected by compact all-in-one weather stations were compared with measurements from the nearest permanent weather station. We also evaluated the reliability of CRONOS sensors by quantifying the percentage of out-of-range or missing data.

Accuracy of the Soil Moisture Data

Soil moisture measured by the CRONOS stations during the winter wheat growing season was typically between 0.20 and 0.40 $cm^3\,cm^{-3}$ with a maximum value of 0.43 $cm^3\,cm^{-3}$ at the Chattanooga site on October 27, 2020 and a minimum of 0.11 at the Chattanooga site on April 13, 2021 (Figure 3). Rainfall events totaling > 50 mm occurred at all three sites in late October 2020, replenishing soil moisture from < 0.20 $cm^3\,cm^{-3}$ to < 0.43 $cm^3\,cm^{-3}$. Soil moisture levels declined through much of November 2020 reaching approximately 0.20 cm^3cm^{-3} at Chickasha

and Chattanooga but remaining somewhat higher at Braman where the crop canopy was less extensive. Winter precipitation events at all sites again replenished the soil moisture levels to near 0.40 cm^3cm^{-3} around mid- February 2021, which is near the time when evaporative demand typically begins to increase from its winter lows and winter wheat typically begins to break dormancy in this region (Sembiring et al., 2000). By mid-April 2021, under the actively growing wheat, soil moisture levels were at or near their minimum values for the season at each site, with the Chattanooga site being the driest. Spring rains and crop senescence contributed to generally greater soil moisture values from mid-April through the end of the season at the Chickasha and Chattanooga sites. In contrast, the Braman site experienced more pronounced periods of soil moisture recharge and late season dry downs in May and June and ended the season with relatively low soil moisture levels. The soil moisture dynamics observed at these three CRONOS sites are consistent with those reported in previous studies monitoring winter wheat fields in Oklahoma (Patrignani and Ochsner, 2018).

The need for cropland soil moisture data is apparent based on the differences between the soil moisture measured at the nearest Mesonet station and that measured at the CRONOS stations (Figure 3). At Chickasha, the Mesonet site only has a soil moisture sensor at the 5-cm depth which is shallower than the effective sensing depth for the CRONOS station. Nevertheless, there is a sharp contrast between the relatively static soil moisture conditions at the Mesonet, site which is dominated by warm season perennial vegetation, and the relatively dynamic soil moisture conditions in the winter wheat cropland, with an NSE of -2.3 between the two stations. The same type of contrast is evident between the Mesonet soil moisture and the CRONOS data at the Chattanooga site, although to a lesser degree with an NSE of -1.4. A negative NSE indicates that the Mesonet soil moisture data provide a poorer estimate of the CRONOS soil moisture dynamics than simply assuming a constant mean value of soil moisture for the entire season. Similar large discrepancies between soil moisture conditions measured by in-situ networks and those measured

under winter wheat have been previously reported (Patrignani and Ochsner, 2018). Interestingly, relatively good agreement existed between the Mesonet soil moisture and the CRONOS soil moisture for the Braman site. This may be related to the fact that the Braman site had minimal winter wheat growth during the fall and winter.

Soil moisture values measured using the cosmic-ray neutron detectors at each site were compared with values determined using soil samples collected regularly throughout the experiment. The MAD between the CRONOS soil moisture estimates and the values determined by soil sampling was 0.022 cm^3cm^{-3}. The NSE was 0.756 and the bias was 0.010 cm^3cm^{-3} (Figure 4). This level of accuracy is comparable to that reported in several previous studies evaluating the cosmic-ray neutron method. For examples, Franz et al. (2016) observed a MAD of 0.0286 cm^3 cm^{-3} when comparing cosmic-ray neutron soil moisture estimates to independent validation data for a cropland site in Austria where the main crop was winter wheat. Similarly, Patrignani et al. (2021) reported a MAD of 0.022 cm^3 cm^{-3} between soil moisture estimates from a lithium foil based cosmic ray neutron detector and independent validation data for a winter wheat site in Kansas, USA. Changes in the winter wheat vegetation water content throughout the season did not appear to affect the accuracy of the CRONOS soil moisture data. The vegetation water contents ranged from 0.116 kg m^{-2} to 1.146 kg m^{-2} over the course of our study (data not shown), and the correlation between the CRONOS soil moisture error and the vegetation water content was not significant ($r = 0.316$, $p = 0.373$). This result is consistent with that of a previous study in winter wheat in which soil moisture estimates from cosmic ray neutron detectors were found to be unaffected by dry above-ground biomass when it was < 1 kg m^{-2} (Patrignani et al., 2021).

Accuracy of the Green Canopy Cover Data

The daily GCC data from the CRONOS stations reveal the seasonal dynamic of the crop growth. Early season growth at the Chickasha and Chattanooga sites produced GCC values >

20% at the start of winter, while slower canopy development at the northernmost site Braman, coupled with left over residue from the prior season, resulted in GCC values < 20% (Figure 5). Essentially no canopy growth was observed at any site December through February, as the wheat passed through its winter dormancy period. That included a period of snow and ice-covered conditions in February 2021, which resulted in GCC values at or near 0. Canopy growth resumed in early March at all three sites but GCC peaked in late March at the Chickasha and Chattanooga sites. From late March to mid-April, GCC slightly declined at Chickasha as soil moisture dropped to 0.16 cm^3cm^{-3}, indicating the likely effects of drought stress. However, rainfall in mid-April replenished soil moisture and led to a secondary peak in GCC in early May. In contrast, at Chattanooga the decline in GCC that was apparently initiated by drought stress starting in late March was not abated by the rainfall and replenished soil moisture in mid-April, rather the decline continued to the end of the season. This can be explained when cross referencing the CRONOS soil water content with the permanent wilting point of the soil at the Chattanooga site (Table 2). The permanent wilting point values were $\geq$ 0.11 cm^3 cm^{-3} across the 0-40 cm soil depth range, and by mid-April, the soil water content at the Chattanooga site had been depleted to 0.10 cm^3 cm^{-3}. Apparently, the spring drought stress effectively terminated the crop. This interaction between the CRONOS soil moisture and GCC variables highlight the value of integrated soil-plant-atmosphere monitoring systems for understanding crop dynamics. At Braman, soil moisture and weather conditions allowed canopy growth to continue until mid-April, after which GCC declined until the end of the season.

The CRONOS GCC values were compared with the average GCC of an approximately 3-ha area surrounding each station for five sampling periods throughout the growing season. The temporal dynamics of the field-scale average GCC were generally well-represented by the CRONOS data, but field-scale average GCC was underestimated by the CRONOS station at the Braman site on four out of five sampling dates (Figure 5). This discrepancy was likely due to the

relatively small footprint of the images from the CRONOS camera and the inherent spatial variability of GCC at the field scale. While we attempted to place the stations in apparently representative locations in the field, the GCC detected by the camera only reflected an area of approximately 6 m^2, whereas the images used to estimate the field-scale GCC were distributed across an area of greater than 30,000 m^2.

In contrast at the Chickasha site, the CRONOS GCC values exhibited a nearly 1:1 relationship with the field-scale GCC data (Figure 6). The MAD between the CRONOS GCC values and the field-scale GCC values was 10.4% at Chickasha, 9.15% at Chattanooga, and 16.6% at Braman. Across all three sites the CRONOS GCC values had a MAD of 12 % from the field-scale average GCC. The CRONOS GCC values also exhibited an NSE of 0.429 and a bias of -4.88 % when compared to the field-scale averages. These results suggest the need to account for a larger area of the field than what was captured by the CRONOS cameras. Analysis of spatial variability of GCC in cropped fields has indicated that anywhere from 4-45 images may be necessary to estimate the field average GCC with ± 5% accuracy (Patrignani and Ochsner, 2015). Aerial images might help to represent the field more holistically if the images maintained adequate spatial resolution (Patrignani and Ochsner, 2015). The implementation of scheduled drone flights or frequent high-resolution satellite images could be potential solutions.

Accuracy of the Weather Data

The CRONOS air temperature observations provide additional context for interpreting the GCC and soil moisture data. At all three sites, daily minimum air temperatures were typically near or below 0˚C from December through February (Figure 7), and the GCC data indicate little or no canopy growth during this period (Figure 5). A severe winter storm in February produced daily maximum temperatures < 0 ˚C for more than a week at each site with complete snow and ice cover and daily minimum temperatures as low as -17.2 ˚C. The melting and infiltration of

frozen precipitation not measured by the CRONOS station apparently led to a substantial increase in soil moisture at the Chattanooga site around this time. By early March, daily maximum air temperature began to regularly exceed 20 ˚C at all three sites, and GCC values began to increase. By the end of the winter wheat growing season, daily maximum temperatures were ≥ 30 ˚C at all three sites.

Daily meteorological measurements made by the CRONOS stations were closely related (NSE ≥ 0.70) to the measurements from the nearest Oklahoma Mesonet stations for all variables except daily maximum relative humidity (Table 3). For example, the daily maximum and minimum air temperatures measured by CRONOS stations and those of the nearest Mesonet stations showed nearly identical ranges and temporal dynamics, including during the period in February 2021 when air temperatures were well below 0 ˚C (Figure 7). The NSE between the CRONOS daily precipitation total and that of the nearest Mesonet station was highest for the Chickasha site (NSE = 0.87) where the distance between the CRONOS station and the Mesonet station was < 1 km. For the other two sites this distance was approximately 17 km and the NSE values were ≤ 0.75. This suggests that some portion of the discrepancy between the CRONOS precipitation data and the Mesonet precipitation data was due to the spatial variability in precipitation and the separation distance between the stations. A similar pattern of lower NSE for more distant stations was evident in the measurements of daily maximum relative humidity, however the maximum humidity's range was narrower than that of most other variables, which tends to lower the NSE value. The standard deviation of the maximum relative humidity was ± 9.3 %. When compared with their nearest Mesonet station, the CRONOS stations on average underestimated the total daily solar radiation (percent bias = -10.6%) and precipitation (-22.3%) and overestimated daily minimum relative humidity (10.5%) and wind speeds (14.9%) (Table 3). A smaller bias for solar radiation was reported in a prior study in Germany, which found that the same all-in-one weather stations underestimated the solar radiation by as much as 3%

(Dombrowski et al., 2021). That study also found that the errors in the precipitation measurements were approximately ± 7.5% and concluded that high winds were to blame. Another study also found that these weather stations tended to slightly overestimate relative humidity (Schunke et al., 2021). Finally, Anand and Molnar, (2018) also reported a substantial overestimation of wind speed (25%) with these weather stations, and noted that the discrepancies were most pronounced at low wind speeds.

Sensor Reliability

To determine the reliability of each measurement type, the percentage of missing or out-of-range data points was determined for each variable (Figure 8). All measurements, except for the images collected for GCC analysis, had error rates less than 2%. Measurements for some variables are dependent on others so that missing or out-of-range, data for one sensor often resulted in errors for more than one variable. For instance, if the relative humidity, atmospheric pressure or air temperature measurement was missing or out-of-range then the vapor pressure or soil moisture could not be calculated by the CRONOS station. Another issue related to the weather station is that the sonic anemometer cannot detect wind speed when its sintered glass reflection plate is covered. Thus, in instances of freezing rain, snow, or rain in high winds the system will not measure the wind speed due to freezing or obstruction. Error rates were far greater for GCC (18.5%) than all other variables, and several factors contributed to these failures. For example, the downward-facing camera orientation allowed for water to collect on and sometimes enter into the cameras, possibly causing malfunctions. Condensation was also observed at times on or in the camera lens, resulting in blurry images and inaccurate GCC estimates. Improvements to the camera housing may be necessary to alleviate issues with water ingress. Other issues were apparently related to the camera hardware or software resulting in failures to collect and transmit images at the scheduled times.

Limitations

The 23-cm long screw anchors used here proved inadequate in some cases when high soil moisture and strong winds caused some of the stations to blow over. Future work should include improving the stability of the CRONOS stations. Another logistical challenge is the requirement for the all-in-one weather station to be leveled. One way we addressed this issue was by making a two-plate leveling system for the weather stations to facilitate precise leveling in the field. To help reduce interference with farm operations we also developed a hinged mast that could fold down, allowing researchers or farm workers to quickly lower the station and pass over it with spray equipment. However, none of the cooperators used this feature, preferring to work around the stations instead. Another practical complication was encountered at the Chattanooga site where cattle were grazing around the station. Cattle panels were placed around the station for protection, but the resulting shadows could affect the GCC measurements. The exclosure also created the potential for the area viewed by the CRONOS camera to be non-representative of the surrounding grazed portion of the field. However, the GCC data appear to show few effects of the exclosure in this case.

CHAPTER IV

CONCLUSION

Farmers and researchers need better ways to monitor cropland soil-plant-atmosphere conditions, and the first generation CRONOS stations introduced here were developed to meet that need. We deployed CRONOS cropland monitoring systems in three winter wheat fields in Oklahoma and compared the resulting soil water content measurements and observed green canopy cover percentages to values determined by independent on-site sampling. We also compared the CRONOS meteorological data with observations from nearby permanent weather stations. The CRONOS soil moisture measurements agreed well with the field-scale validation samples with a MAD of 0.022 cm^3cm^{-3}. The green canopy cover values measured by the CRONOS stations showed good agreement with the field-scale average green canopy cover at two out of three locations. At one location, the small footprint of the CRONOS camera and the spatial variability of the crop canopy resulted in the CRONOS green canopy cover values consistently underestimating the field-scale average. The CRONOS observations of air temperature and atmospheric pressure showed excellent agreement with those from the nearest permanent weather station (NSE $\geq$ 0.93), but other variables, showed poorer agreement with underestimates for precipitation and solar radiation and overestimates for daily minimum relative humidity and daily average wind speed. The reliability of the CRONOS stations was generally high, with <2%of missing or out-of-range data, except for the digital photos used to estimate

GCC, which had missing data 18.5% of the time.

These first-generation CRONOS stations represent an important step toward enabling researchers and farmers to more effectively monitor the soil-plant-atmosphere continuum in cropland, paving the way for the development of improved models and management plans based on in-situ data. In this way, the CRONOS systems will not only help researchers accurately track soil-plant-atmosphere dynamics in the field but may also allow farmers to better estimate yield potentials mid-season leading to more effective tactical management decisions and protecting against monetary and environmental losses due to under- or over-application of fertilizers or other inputs. For subsequent generations of CRONOS stations, development efforts should focus on identifying lower cost neutron detectors, better anchoring systems, and more reliable and representative vegetation monitoring.

REFERENCES

Anand, M., and P. Molnar. 2018. Performance of TAHMO Zurich Weather Station. Institute of Environmental Engineering, D-Baug: ETH Zurich, Switzerland.

Andreasen, M., K.H. Jensen, D. Desilets, T.E. Franz, M. Zreda, et al. 2017. Status and Perspectives on the Cosmic-Ray Neutron Method for Soil Moisture Estimation and Other Environmental Science Applications. Vadose Zone Journal 16(8): vzj2017.04.0086. doi: 10.2136/vzj2017.04.0086.

Badiee, A., J.R. Wallbank, J.P. Fentanes, E. Trill, P. Scarlet, et al. 2021. Using Additional Moderator to Control the Footprint of a COSMOS Rover for Soil Moisture Measurement. Water Resources Research 57(6): e2020WR028478. doi: 10.1029/2020WR028478.

Campbell Scientific. 2019. ClimaVUE 50 Product Manual. https://s.campbellsci.com/documents/au/manuals/climavue50.pdf (accessed 6 April 2022).

Colliander, A., Z. Yang, R. Mueller, A. Sandborn, R. Reichle, et al. 2019. Consistency Between NASS Surveyed Soil Moisture Conditions and SMAP Soil Moisture Observations. Water Resources Research 55(9): 7682–7693. doi: 10.1029/2018WR024475.

Desilets, D., M. Zreda, and T.P.A. Ferré. 2010. Nature's neutron probe: Land surface hydrology at an elusive scale with cosmic rays. Water Resources Research 46(11). doi: https://doi.org/10.1029/2009WR008726.

Dombrowski, O., H.-J. Hendricks Franssen, C. Brogi, and H.R. Bogena. 2021. Performance of the ATMOS41 All-in-One Weather Station for Weather Monitoring. Sensors 21(3): 741. doi: 10.3390/s21030741.

Franz, T.E., A. Wahbi, M. Vreugdenhil, G. Weltin, L. Heng, et al. 2016. Using Cosmic-Ray Neutron Probes to Monitor Landscape Scale Soil Water Content in Mixed Land Use Agricultural Systems. Applied and Environmental Soil Science 2016: e4323742. doi: 10.1155/2016/4323742.

Gavlak, R., D. Horneck, R.O. Miller, and J. Kotuby-Amacher. 2003. Soil, plant and water reference methods for the western region. WCC-103 Publication, Fort Collins, CO.

Iwema, J., M. Schrön, J. Koltermann Da Silva, R. Schweiser De Paiva Lopes, and R. Rosolem. 2021. Accuracy and precision of the cosmic-ray neutron sensor for soil moisture estimation at humid environments. Hydrological Processes 35(11): e14419. doi: 10.1002/hyp.14419.

Köhli, M., M. Schrön, M. Zreda, U. Schmidt, P. Dietrich, et al. 2015. Footprint characteristics revised for field-scale soil moisture monitoring with cosmic-ray neutrons. Water Resources Research 51(7): 5772–5790. doi: 10.1002/2015WR017169.

Krueger, E.S., T.E. Ochsner, M.R. Levi, J.B. Basara, G.J. Snitker, et al. 2021. Grassland productivity estimates informed by soil moisture measurements: Statistical and mechanistic approaches. Agronomy Journal 113(4): 3498–3517. doi: 10.1002/agj2.20709.

Madsen, H.B., C.R. Jensen, and T. Boysen. 1986. A comparison of the thermocouple psychrometer and the pressure plate methods for determination of soil water characteristic curves. Journal of Soil Science 37(3): 357–362. doi: 10.1111/j.1365-2389.1986.tb00368.x.

McCuen, R.H., Z. Knight, and A.G. Cutter. 2006. Evaluation of the Nash–Sutcliffe Efficiency Index. Journal of Hydrologic Engineering 11(6): 597–602. doi: 10.1061/(ASCE)1084-0699(2006)11:6(597).

McPherson, R.A., C.A. Fiebrich, K.C. Crawford, J.R. Kilby, D.L. Grimsley, et al. 2007. Statewide Monitoring of the Mesoscale Environment: A Technical Update on the Oklahoma Mesonet. Journal of Atmospheric and Oceanic Technology 24(3): 301–321. doi: 10.1175/JTECH1976.1.

Ochsner, E., M.H. Cosh, R. Cuenca, H.D. R, S.D. C, et al. 2013. State of the art in large-scale soil moisture monitoring. Soil Science Society of America Journal: 1. doi: 10.2136/sssaj2013.03.0093.

Oklahoma. 2022. Oklahoma Climatological Survey. https://climate.ok.gov/index.php (accessed 6 April 2022).

Patrignani, A., and T.E. Ochsner. 2015. Canopeo: A Powerful New Tool for Measuring Fractional Green Canopy Cover. Agronomy Journal 107(6): 2312–2320. doi: https://doi.org/10.2134/agronj15.0150.

Patrignani, A., and T.E. Ochsner. 2018. Modeling transient soil moisture dichotomies in landscapes with intermixed land covers. Journal of Hydrology 566: 783–794. doi: 10.1016/j.jhydrol.2018.09.049.

Patrignani, A., T.E. Ochsner, B. Montag, and S. Bellinger. 2021. A Novel Lithium Foil Cosmic-Ray Neutron Detector for Measuring Field-Scale Soil Moisture. Frontiers in Water 3. https://www.frontiersin.org/article/10.3389/frwa.2021.673185 (accessed 22 June 2022).

Pereira, L.S., P. Paredes, F. Melton, L. Johnson, T. Wang, et al. 2020. Prediction of crop coefficients from fraction of ground cover and height. Background and validation using ground and remote sensing data. Agricultural Water Management 241: 106197. doi: 10.1016/j.agwat.2020.106197.

Quiring, S.M., T.W. Ford, J.K. Wang, A. Khong, E. Harris, et al. 2016. The North American Soil Moisture Database: Development and Applications. Bulletin of the American Meteorological Society 97(8): 1441–1459. doi: 10.1175/BAMS-D-13-00263.1.

Rosolem, R., W.J. Shuttleworth, M. Zreda, T.E. Franz, X. Zeng, et al. 2013. The Effect of Atmospheric Water Vapor on Neutron Count in the Cosmic-Ray Soil Moisture Observing System. Journal of Hydrometeorology 14(5): 1659–1671. doi: 10.1175/JHM-D-12-0120.1.

Rossel, F., and J. Garbrecht. 1999. Variability Characteristics of Monthly Precipitation in Central Oklahoma1. JAWRA Journal of the American Water Resources Association 35(6): 1455–1461. doi: 10.1111/j.1752-1688.1999.tb04229.x.

Sapundjiev, D., T. Verhulst, and S. Stankov. 2020. Chapter 20 - International Database of Neutron Monitor Measurements: Development and Applications. In: Škoda, P. and Adam, F., editors, Knowledge Discovery in Big Data from Astronomy and Earth Observation. Elsevier. p. 371–383

Savitzky, A., and M.J. Golay. 1964. Smoothing and differentiation of data by simplified least squares procedures. Analytical chemistry 36(8): 1627–1639.

Schunke, J., P. Laux, J. Bliefernicht, M. Waongo, W. Sawadogo, et al. 2021. Exploring the Potential of the Cost-Efficient TAHMO Observation Data for Hydro-Meteorological Applications in Sub-Saharan Africa. Water 13(22): 3308. doi: 10.3390/w13223308.

Sembiring, H., H.L. Lees, W.R. Raun, G.V. Johnson, J.B. Solie, et al. 2000. Effect of growth stage and variety on spectral radiance in winter wheat. Journal of Plant Nutrition 23(1): 141–149. doi: 10.1080/01904160009382003.

Soil Survey Staff, N.R.C.S. 2022. Web Soil Survey. http://websoilsurvey.sc.egov.usda.gov (accessed 6 April 2022).

Wyatt, B.M., T.E. Ochsner, C.A. Fiebrich, C.R. Neel, and D.S. Wallace. 2017. Useful Drainage Estimates Obtained from a Large-Scale Soil Moisture Monitoring Network by Applying the Unit-Gradient Assumption. Vadose Zone Journal 16(6): vzj2017.01.0016. doi: 10.2136/vzj2017.01.0016.

Wyatt, B.M., T.E. Ochsner, E.S. Krueger, and E.T. Jones. 2020. In-situ soil moisture data improve seasonal streamflow forecast accuracy in rainfall-dominated watersheds. Journal of Hydrology 590: 125404. doi: 10.1016/j.jhydrol.2020.125404.

Yimam, Y.T., T.E. Ochsner, and V.G. Kakani. 2015. Evapotranspiration partitioning and water use efficiency of switchgrass and biomass sorghum managed for biofuel. Agricultural Water Management 155: 40–47. doi: 10.1016/j.agwat.2015.03.018.

Zhang, Y., T.E. Ochsner, C.A. Fiebrich, and B.G. Illston. 2019. Recalibration of Sensors in One of The World's Longest Running Automated Soil Moisture Monitoring Networks. Soil Science Society of America Journal 83(4): 1003–1011. doi: 10.2136/sssaj2018.12.0481.

Zreda, M., W.J. Shuttleworth, X. Zeng, C. Zweck, D. Desilets, et al. 2012. COSMOS: the COsmic-ray Soil Moisture Observing System. Hydrology and Earth System Sciences 16(11): 4079–4099. doi: https://doi.org/10.5194/hess-16-4079-2012.

APPENDICES

Table 1. Agronomic and climatological data for each site where CRONOS stations were deployed.

Site	Planting date	Annual precipitation	Mean Annual Temperature
		mm	˚C
Chickasha	October 10, 2020	876	15.8
Chattanooga	September 24, 2020	709	16.3
Braman	October 8, 2020	734	14.7

Table 2. The average bulk density, porosity, and volumetric water content at wilting point (-1500 kPa) at each depth, for each CRONOS site.

Site	ρ_b	ε	-1500 kPa
	g cm^{-3}	cm^3 cm^{-3}	cm^3 cm^{-3}
0-5 cm			
Chickasha	1.38	0.48	0.10
Chattanooga	1.34	0.49	0.11
Braman	1.35	0.49	0.09
5-10 cm			
Chickasha	1.53	0.42	0.12
Chattanooga	1.55	0.41	0.13
Braman	1.57	0.40	0.12
10-40 cm			
Chickasha	1.56	0.41	0.15
Chattanooga	1.55	0.41	0.18
Braman	1.53	0.42	0.14

Table 3. The MAD, NSE, and percent bias of each CRONOS station variable when compared to the nearest Oklahoma Mesonet station on a by variable basis. θ is the soil moisture, and P is the sum of daily precipitation. T_{max} and T_{min} are the daily maximum and minimum temperature. R_s is the daily sum of the solar flux density. RH_{max} and RH_{min} are the daily max and minimum relative humidity observed. P_a is the atmospheric pressure. u_2 is the daily average wind speed and Dis. indicates the distance between the CRONOS and Mesonet stations.

	Site	θ	P	T_{max}	T_{min}	R_s	RH_{max}	RH_{min}	P_a	u_2	Dis.
MAD		$cm^3\ cm^{-3}$	mm	˚C	˚C	MJ m^{-2}	%	%	kPa	m s^{-1}	km
	Chickasha	0.12	1.56	0.60	0.01	1.6	2.88	8.16	0.06	0.67	0.14
	Chattanooga	0.11	2.47	0.81	0.79	1.6	3.28	4.48	0.16	0.61	17.6
	Braman	0.03	2.46	0.73	1.04	1.4	4.49	5.51	0.03	0.58	17.3
NSE											
	Chickasha	-2.3	0.87	0.99	0.95	0.89	0.73	0.78	0.99	0.73	0.14
	Chattanooga	-1.4	0.70	0.99	0.98	0.93	0.67	0.92	0.93	0.72	17.6
	Braman	0.70	0.75	0.99	0.98	0.94	0.34	0.88	0.99	0.78	17.3
Percent Bias		%	%	%	%	%	%	%	%	%	
	Chickasha	-39.8	-18.6	-3.09	16.2	-12.8	1.37	14.6	-0.05	19.3	0.14
	Chattanooga	-41.2	-17.5	-3.95	4.72	-10.2	0.19	7.99	-0.16	11.0	17.6
	Braman	-0.78	-30.8	-3.58	18.3	-8.68	-3.51	9.05	-0.01	14.4	17.3

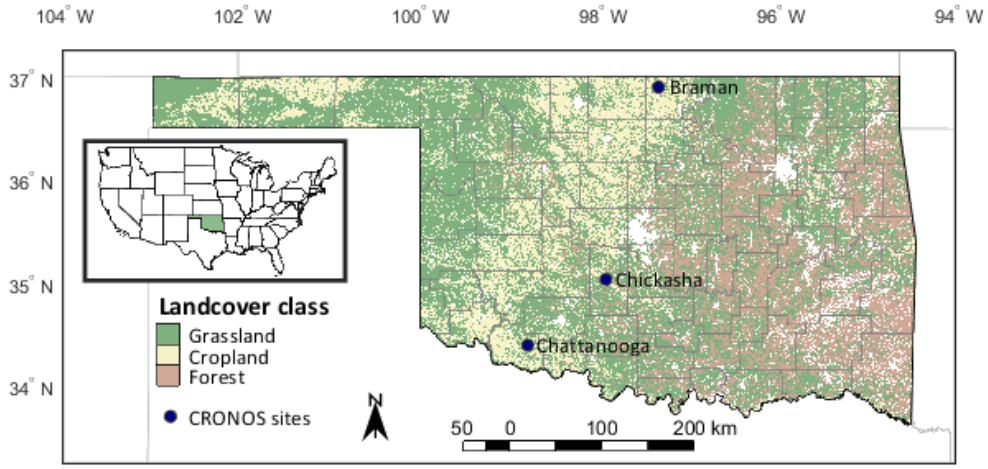

Figure 1. The location of the three CRONOS sites utilized in this study. The small inlaid map shows Oklahoma's location within the United States and the coloration of the map indicates the predominant land cover type throughout the state. The CRONOS stations are distributed so that they span much of the winter wheat growing region of Oklahoma.

Figure 2. Photograph of CRONOS station 2 located in Tillman County, Oklahoma near the town of Chattanooga. This station is equipped with an all-in-one weather station (top), digital camera (arm), and cosmic ray neutron detector (box) which is located behind the data logger (box).

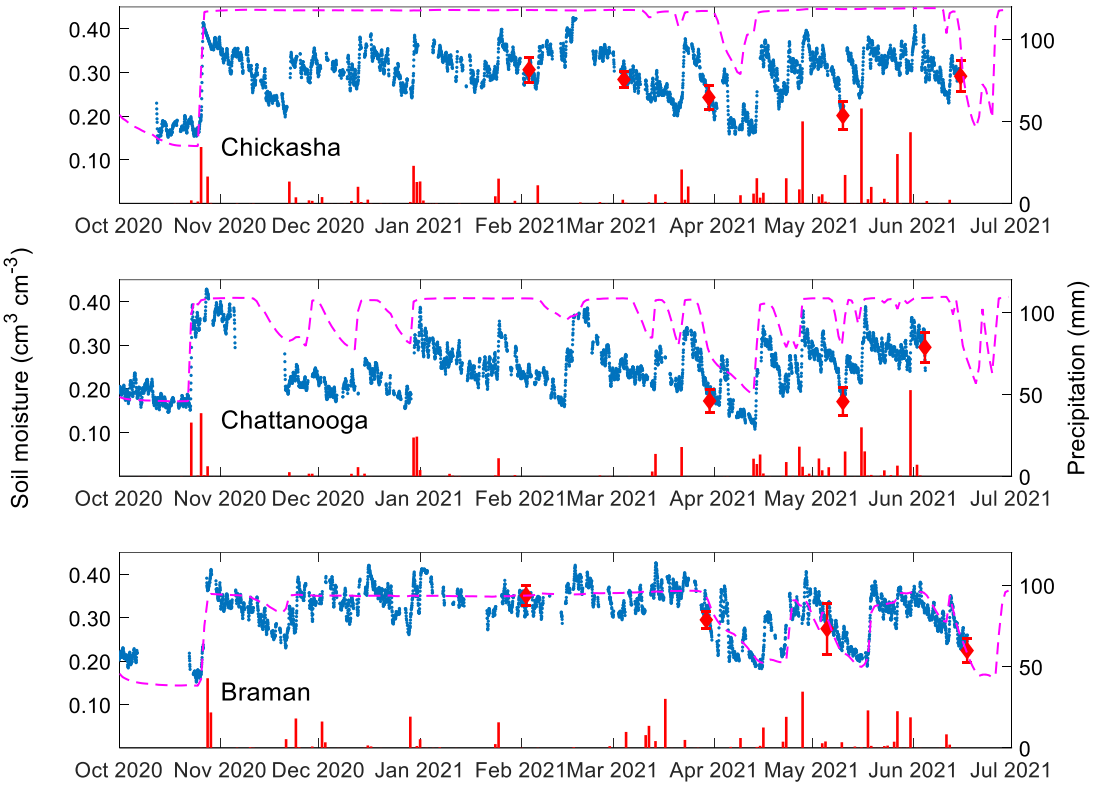

Figure 3. Time series of the smoothed hourly soil moisture (cm^3cm^{-3}) from each CRONOS station during the 2020-2021 winter wheat growing season (blue dots). The red diamonds represent the distance- and depth-weighted average soil moisture of the field as determined by periodic soil sampling. The error bars on the diamonds are the depth-weighted standard deviations of the 14 samples in each depth layer (0-5, 5-10, 10-40 cm) that were used to calculate the field average. The dashed magenta line represents the depth-weighted daily soil moisture measured at the Mesonet site nearest to each CRONOS station. The red bars at the base of each plot represent CRONOS daily precipitation totals throughout the course of the growing season.

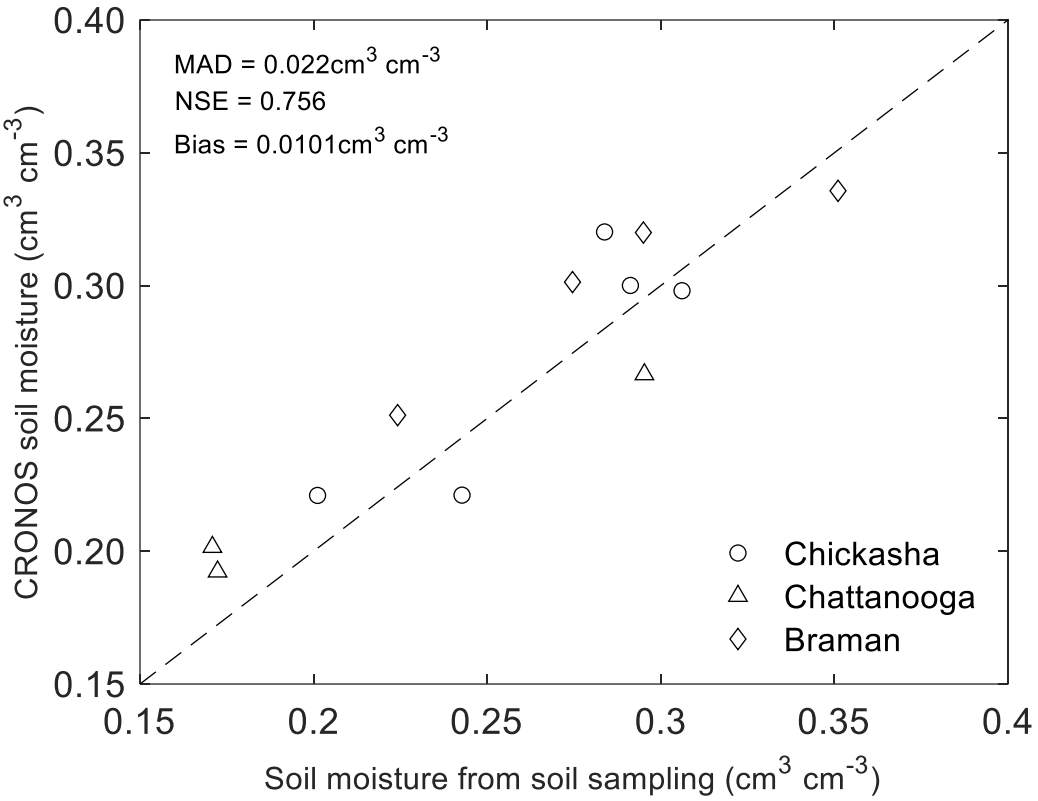

Figure 4. CRONOS soil moisture data versus field-scale average soil moisture estimated based on soil samples collected at different times throughout the growing season at a total of 14 locations on concentric circles with radii of 5, 50, and 100 m around the CRONOS station. The CRONOS data are the mean of the 4 hours after the start of soil sampling, and the hourly data were smoothed with a Savitzky-Golay filter. The soil moisture values for each soil sampling location and depth (0-5, 5-10, 10-40 cm) were weighted according to the procedure of Köhli et al. (2015) to calculate the field-scale average.

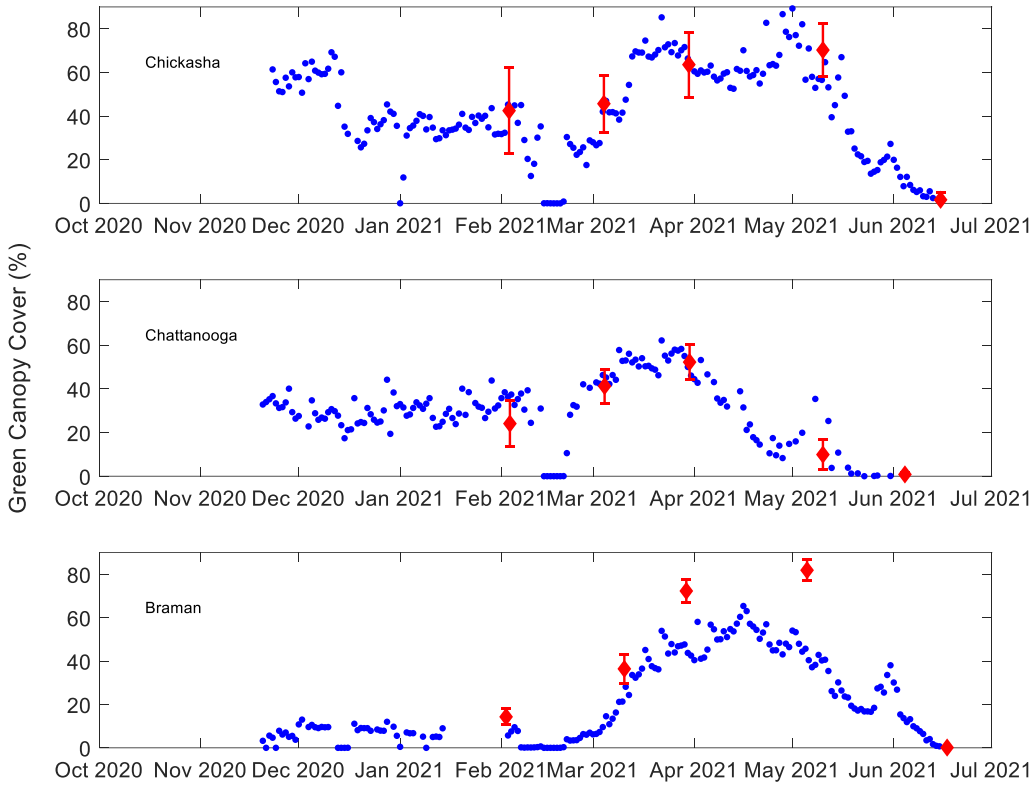

Figure 5. Daily average green canopy cover (GCC) measured using photos from a digital camera mounted on the CRONOS station. The photos were processed using the Canopeo algorithm (Patrignani and Ochsner, 2015) to determine GCC. The red diamonds are the field-scale average GCC based on 14 photographs taken at the soil sampling locations using a smartphone. Images were processed by the Canopeo smartphone application and the red error bars represent the standard deviation of that dataset.

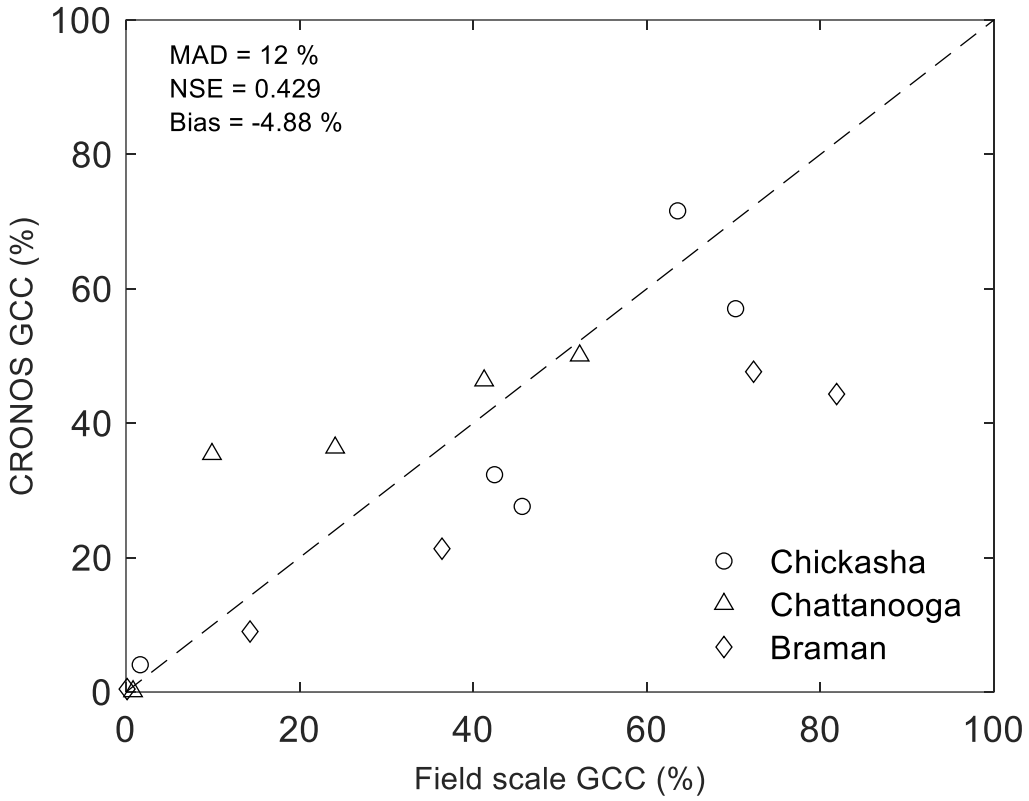

Figure 6. CRONOS green canopy cover (GCC) estimate plotted against the field-scale average GCC based on measurements at 14 locations in each field on five dates throughout the growing season. The CRONOS GCC values are the average GCC for the photos collected by the station at five times (09:00, 11:00, 13:00, 15:00, and 17:00) on the day of sampling. The MAD, NSE, and bias across all three sites are displayed in the top left corner.

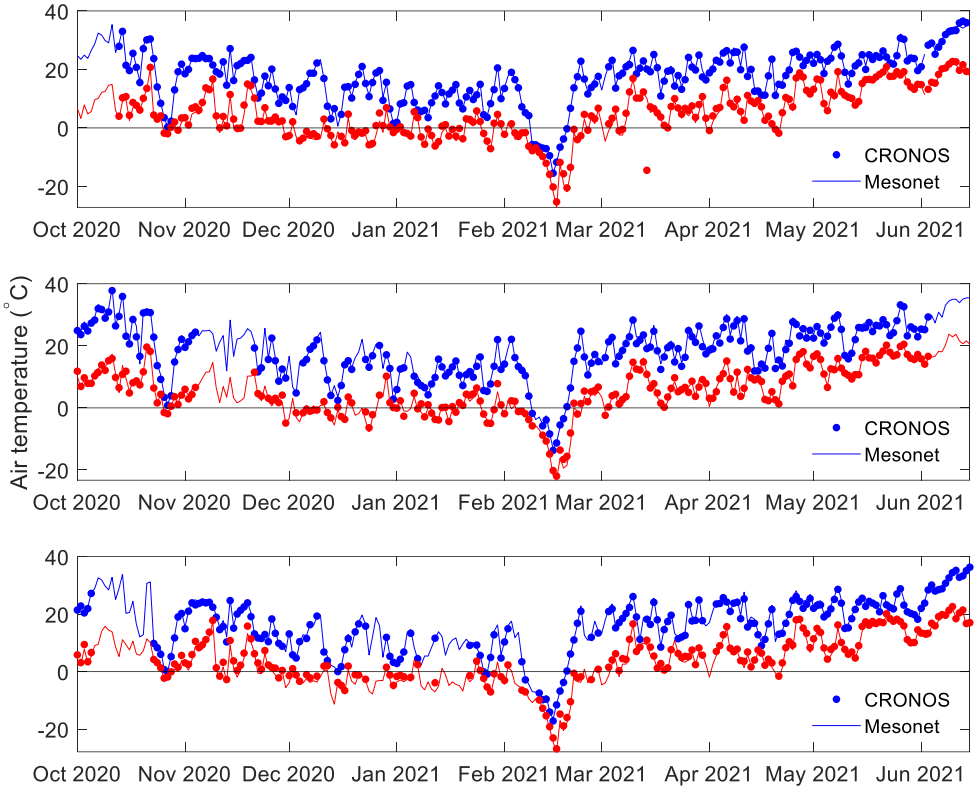

Figure 7. Time series of daily maximum (blue) and minimum (red) air temperatures at each CRONOS station, along with the daily maximum and minimum air temperature measured by the closest station of the Oklahoma Mesonet.

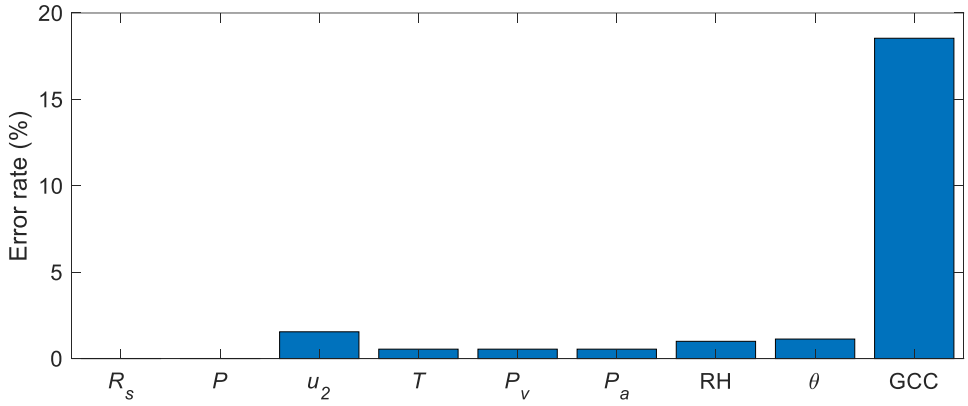

Figure 8. Percent of missing or invalid sub-daily observations for CRONOS atmospheric variables, GCC readings, and soil moisture (θ) measurements across three sites in Oklahoma during the 2020-2021 winter wheat growing season. P is precipitation. T air temperature. R_s is solar radiation. RH is relative humidity. P_a is atmospheric pressure. P_v is vapor pressure. u_2 is wind speed at 2 m, and GCC is the green canopy cover

VITA

Denton Cole Diggins

Candidate for the Degree of

Master of Science

Thesis: CROPLAND OBSERVATORY NODES (CRONOS): PORTABLE, INTEGRATED SOIL-PLANT-ATMOSPHERE MONITORING SYSTEMS

Major Field: Plant and Soil Sciences

Biographical:

Education:

- Completed the requirements for the Master of Science in Plant and Soil Sciences at Oklahoma State University, Stillwater, Oklahoma in July, 2022.
- Completed the requirements for the Bachelor of Science in Soil, Environmental, and Atmospheric Sciences at the University of Missouri, Columbia, Missouri in 2020.
- Completed the requirements for the Minor of Science in Plant Sciences at the University of Missouri, Columbia, Missouri in 2020.
- Completed the requirements for a Certification in Geographic Information Systems at the University of Missouri, Columbia, Missouri in 2020.

Experience:

- Former student researcher at the University of Missouri
- Professional Memberships:
- ASA-CSSA-SSSA member
- McNair Scholar
- Coca Cola Scholar